ACS APPLIED MATERIALS & INTERFACES

Research Article

www.acsami.org

Bright and Stable CdSe/CdS@SiO_2 Nanoparticles Suitable for Long-Term Cell Labeling

Tangi Aubert,*[,†,‡] Stefaan J. Soenen,[‡,§,⊥] Daniel Wassmuth,[†,‡] Marco Cirillo,[†,‡] Rik Van Deun,[#] Kevin Braeckmans,[‡,§] and Zeger Hens*[,†,‡]

[†]Physics and Chemistry of Nanostructures, Ghent University, Krijgslaan 281-S3, 9000 Ghent, Belgium

[§]Laboratory of General Biochemistry and Physical Pharmacy, Ghent University, Harelbekestraat 72, 9000 Ghent, Belgium

[#]L^3 – Luminescent Lanthanide Lab, f-element coordination chemistry, Ghent University, Krijgslaan 281-S3, 9000 Ghent, Belgium

[‡]Center for Nano- and Biophotonics (NB-Photonics), Ghent University, 9000 Ghent, Belgium

Supporting Information

ABSTRACT: We report on the synthesis of luminescent CdSe/CdS@SiO_2 nanoparticles and their application to cell labeling. The main novelty of these nanoparticles is the use of newly developed "flash" CdSe/CdS quantum dots (QDs), which are obtained through a new fast and efficient synthesis method recently reported. These core–shell QDs are encapsulated in silica nanoparticles through a water-in-oil microemulsion process, resulting in CdSe/CdS@SiO_2 nanoparticles with good morphology and controlled architecture. The main asset of these luminescent nanoparticles is their high photoluminescent quantum yield, which is equal to that of the original CdSe/CdS QDs and remains unchanged even after several months of storage in water. Thanks to the remarkable stability of their optical property in aqueous environment and to their low levels of toxicity, the high potential of these nanoparticles for long-term cell labeling is demonstrated.

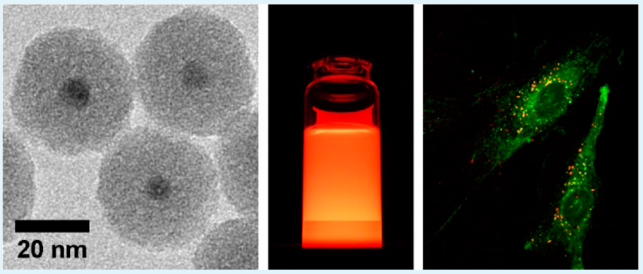

KEYWORDS: *quantum dots, fluorescent, microemulsion, bioimaging, theranostics*

1. INTRODUCTION

The use of functional nanoparticles in the fields of biotechnology, medical diagnostic, and therapy techniques has raised an increasing interest in the past years.[1−3] Luminescent nanoparticles in particular are very useful for bioimaging and cell labeling. For these applications, semiconductor quantum dots (QDs) are an attractive alternative for classic organic fluorophores as light emitters because they exhibit a higher brightness thanks to large absorption cross-sections, a tunable narrow emission spectrum and a broadband absorption spectrum.[4] Therefore, QDs are ideal potential nanoprobes for sensitive and long-term multiplexed bioimaging and biosensing.[5−7]

For optimal properties, colloidal QDs are best synthesized at relatively high temperature (up to 350 °C) in apolar solvents. To be used in bioimaging, they should thus be transferred to biological media such as water or buffer solutions. For this purpose, the encapsulation of QDs in silica nanoparticles has been investigated in the past years.[8−12] Indeed, a silica matrix can provide nanocrystals with an enhanced colloidal stability in polar solvents and for a wide range of conditions (pH, ionic strength).[13] In addition, silica is a relatively biocompatible material and its surface can be functionalized with a wide range of groups, including amines and thiols,[14] that can thereafter be used for coupling the nanoparticles with biomolecules of interest and for specific targeting of cells or intracellular structures.[2,15]

Unfortunately, the properties of semiconductor QDs can quickly deteriorate in strongly oxidative environments such as water, which therefore limits their use in biological applications. In solution, reactive oxygen species (ROS) such as oxygen superoxide or singlet oxygen can cause photooxidation of the QDs resulting in serious deterioration of their optical properties, with in particular a decrease of their photoluminescence quantum yield (PLQY).[16−18] In the same way, the degradation of QDs can result in the release of toxic elements such as Cd^{2+} ions, a known heavy metal toxicant.[19−21] These issues were so far not fully solved by the encapsulation of the QDs in silica nanoparticles because of the high porosity of the silica matrix made by sol–gel approaches. Furthermore, in studies on the encapsulation of QDs in silica nanoparticles the effect of the process on the PLQY is not rigorously analyzed. The reported values are often obtained by measurements relative to a dye with a known PLQY, whereas this method cannot be accurate due to the scattering of light by such silica coated nanoparticles. In addition, the PLQY values are typically reported for freshly prepared samples and the long-term

Received: April 24, 2014
Accepted: June 23, 2014
Published: June 23, 2014

stability of the PLQY of QD@SiO_2 nanoparticles is usually not addressed. Thus, in addition to the long lasting problem of QD degradation, which has always limited their true application to bioimaging, the accurate monitoring of this degradation is also an open challenge.

In this study, we overcome most of these limitations by the silica encapsulation of newly developed "flash" CdSe/CdS QDs, which are obtained through a very fast and efficient method we recently reported.[22] These "flash" QDs meet with state-of-the-art criteria of quality in terms of morphology and optical properties for such core−shell heterostructures, including good size monodispersity, narrow emission spectra, high PLQYs, and a low blinking behavior, which are essential properties for biolabeling applications. In a second step, these QDs were encapsulated in silica nanoparticles through a water-in-oil microemulsion process, a very powerful tool for the synthesis of functional silica nanoparticles with complex architectures and with sizes below 50 nm,[23] which has already been successfully employed for the silica encapsulation of hydrophobic nanocrystals, including semiconductor QDs,[10−12] but also anisotropic nanorods.[24] The effect of the silica encapsulation and the subsequent transfer of the nanoparticles into water on the PLQY of the QDs was carefully investigated by using an integrating sphere and an improved calculation method as detailed in the Experimental Section and in the Supporting Information. With this method, we demonstrate the high physicochemical stability of these "flash" CdSe/CdS@SiO_2 nanoparticles. Opposite from QDs synthesized using a classical "SILAR" approach,[25] they fully retain their PLQY even after long-term storage in water and exhibit a high photostability under continuous UV irradiation. This enhanced stability and its careful monitoring represent considerable improvements to the field of QD@SiO_2 nanoparticles and constitutes the major novelty of this work. In addition, the cytotoxic effects of the CdSe/CdS@SiO_2 nanoparticles were investigated according to previously optimized methods for nanocytotoxicity evaluation,[26] proving effective protection against acute toxicity by the silica coating. Finally, taking the advantage of the high stability of their optical properties and their reduced toxicity, the usefulness of these nanoparticles for cell labeling in terms of particle uptake and long-term cell visualization is evidenced. We thus demonstrate that the combination of "flash" CdSe/CdS QDs and a microemulsion-based silica coating yields nanoparticles with a high physicochemical stability and photostability but also with a low toxicity. These results truly defeat the limitations restricting the bioapplications of QDs. This considerable breakthrough will pave the way for the development of efficient nanoprobes for long-term cell tracking and labeling, but also for the further development of complex multifunctional nanoparticles.

2. EXPERIMENTAL SECTION

2.1. Chemicals. Cadmium oxide (CdO, 99.998% Puratronic) and trioctylphosphine oxide (TOPO, 98%) were purchased from Alfa-Aesar. Octadecylphosphonic acid (ODPA, 98%) was purchased from PCI. Trioctylphosiphine (TOP, 97%) and sulfur powder (S, 99.999%) were purchased from Strem. Selenium powder (Se, 99.999%), oleic acid (OA, 90%), tetraethyl orthosilicate (TEOS, 98%) and polyoxyethylene (4) lauryl ether (Brij30) were purchased from Sigma-Aldrich. *n*-Heptane (99.9%) was purchased from VWR. Ammonia solution (28−30% in water) was purchased from Merck.

2.2. Synthesis of the "Flash" CdSe/CdS QDs. The "flash" CdSe/CdS QDs were synthesized according to a method we recently reported.[22] First, 4 nm sized wurtzite CdSe cores were prepared according to a procedure described in the literature.[27] Briefly, 0.06 g of CdO, 3 g of TOPO, and 0.280 g of ODPA were mixed in a 25 mL three neck flask. The mixture was heated to 150 °C under a vacuum for 1 h. The solution was then put under a nitrogen atmosphere and heated to 345 °C. Next, 1.8 mL of TOP were injected. After the temperature had recovered, a solution containing 0.058 g of Se dissolved in 0.360 g of TOP was injected. The reaction time was adapted to obtain CdSe QDs of 4 nm in size and the QDs were purified by several cycles of precipitation, centrifugation and resuspension. Next, the CdSe/CdS core−shell QDs were obtained through a seeded growth approach using the previously mentioned wurtzite CdSe QDs as cores. For this synthesis, 0.08 g of CdO and 1.6 g of oleic acid were mixed with 3 g of TOPO in a 25 mL three neck flask. The reaction mixture was heated to 120 °C while flushing with nitrogen for 1 h. The temperature was then increased to 330 °C. As soon as the solution became colorless, 1.8 mL of TOP were injected. After the temperature had recovered, 1.8 mL of a solution containing 87 nmol of CdSe core QDs and 0.06 g of S in TOP were injected. After 3 min, the reaction was quenched by a sudden drop of the temperature using a water bath, followed by the injection of 10 mL of toluene. The nanocrystals were purified by the addition of isopropanol and methanol, centrifugation and redispersion in toluene. The purification was repeated three times.

2.3. Synthesis of the CdSe/CdS@SiO_2 Nanoparticles. The above-mentioned CdSe/CdS QDs were encapsulated in silica nanoparticles through a water-in-oil microemulsion process. For this, 25 nmol of CdSe/CdS QDs was mixed in 50 mL of heptane and 16 mL of Brij30. After 15 min of stirring, 2.5 mL of Milli-Q water and 0.5 mL of ammonia solution were added dropwise. After 1 h of stirring to ensure stability and homogeneity of the microemulsion, 1.5 mL of TEOS were added. The reaction was left under stirring for 3 days, then the microemulsion was precipitated by addition of a large volume of ethanol (∼30 mL) and the nanoparticles were collected by centrifugation (relative centrifugal force, RCF = 3000 g, 5 min). The nanoparticles were purified by repeated centrifugation cycles in Milli-Q water (RCF = 10 000 g, 30 min) and finally redispersed in Milli-Q water. The pH of the QD@SiO_2 nanoparticles solution was always comprised between 8 and 9.

2.4. Characterization Techniques. Bright-field transmission electron microscopy (TEM) images were taken using a Cs-corrected JEOL 2200 FS microscope. Photoluminescence measurements were done on an Edinburgh Instruments FLSP920 UV−vis−NIR spectrofluorimeter, using a 450W xenon lamp as the excitation source. The signals were collected with a Hamamatsu R928P PMT detector, which has a response curve between 200 and 900 nm. All emission spectra were recorded for an excitation wavelength of 365 nm and were corrected for the detector sensitivity. The PLQY of the QD@SiO_2 nanoparticles were measured for an excitation wavelength of 365 nm and by using an integrating sphere. The measurement method for measuring the absolute PLQY of these nanoparticles was adapted from the method described by Mello et al.[28] which was improved in order to correct the measurements for the reflection on the cuvette inside the integrating sphere (see the Supporting Information for a complete description of the method and calculation details).

2.5. Toxicity and Cell Labeling Studies. All toxicity and cell labeling studies were performed using primary human umbilical vein endothelial cells (HUVEC) as a representative cell model for both in vitro and in vivo evaluation of nanoparticle toxicity.[29] For these studies, the concentration in nanoparticles was estimated by weighing a dried extract of the initial solution and by assuming a density of 2 for silica. A full methodology on cell culture protocols and detailed experimental protocols on cell labeling studies can be found in the Supporting Information that accompanies this article.

3. RESULTS AND DISCUSSION

3.1. Structure and Morphology. *3.1.1. "Flash" CdSe/CdS QDs and CdSe/CdS@SiO_2 Nanoparticles.* One of the main advantages of the "flash" synthesis is the possibility to grow relatively thick CdS shells in no more than 3 min of reaction.

The "flash" CdSe/CdS QDs synthesized according to the procedure described in the Experimental Section are 9.5 ± 1.2 nm in size (Figure 1a), which corresponds to about 8 layers of CdS. As demonstrated elsewhere,[22] with this synthesis method the CdS shell grows epitaxially on the wurtzite CdSe cores and the CdSe/CdS QDs also have a wurtzite structure. Through the microemulsion process the QDs were successfully encapsulated in silica nanoparticles (Figure 1b). The CdSe/CdS@SiO_2 nanoparticles show a good morphology with more than 99% of them having one single QD perfectly in its center and surrounded by a homogeneous silica layer. The CdSe/CdS@SiO_2 nanoparticles have an average diameter of 33.8 ± 2.8 nm, corresponding to a silica shell thickness of about 12 nm.

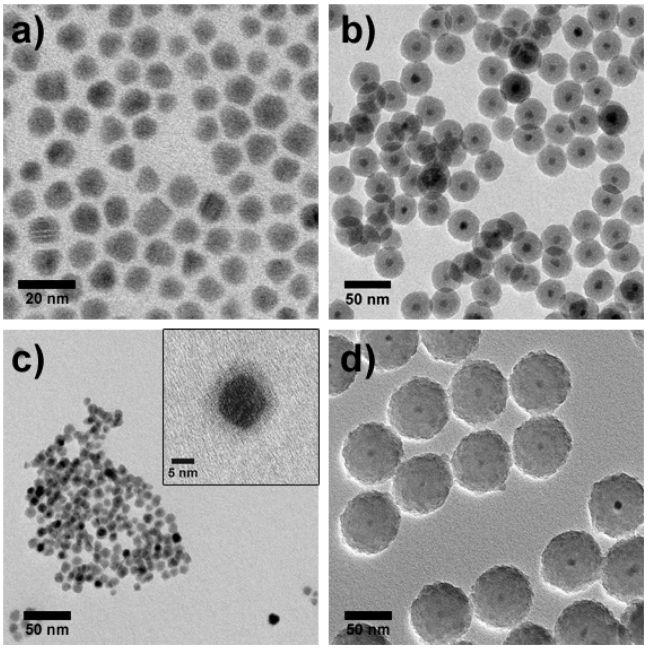

Figure 1. TEM images of (a) the CdSe/CdS QDs, (b) the CdSe/CdS@SiO_2 nanoparticles obtained as described in the Experimental Section, and the CdSe/CdS@SiO_2 nanoparticles obtained by using either (c) 40 times less or (d) 25 times more silica precursor.

3.1.2. Tuning the Silica Shell Thickness. Being able to control the size of the nanoparticles is an important parameter when developing tools for biotechnology applications. With this microemulsion technique, the thickness of the silica shell could be easily tuned in a wide range of sizes just by varying the amount of silica precursor (TEOS) in the synthesis. Indeed, as demonstrated by other authors,[10,11] in a water-in-oil microemulsion, hydrophobic nanocrystals capped with amphiphilic ligands act as nucleation centers for the growth of the silica nanoparticles. During this process, both the nanocrystals and the silica precursor are initially located in the oil phase. The amphiphilic ligands are exchanged by hydrolyzed silica monomers, and the nanocrystals can then migrate to the aqueous inverted micelles where the growth of the silica shell will proceed.[10,11] As a result of this mechanism, each QD@SiO_2 nanoparticle contains only one single QD core, and thanks to the full chemical yield of the silica formation there is a direct linear relationship between the amount of TEOS involved in the synthesis and the volume of the silica shell per nanoparticle. For illustration, images c and d in Figure 1 show CdSe/CdS@SiO_2 nanoparticles with silica shell thicknesses of less than 2 nm and more than 30 nm respectively, which were obtained by using either 40 times less or 25 times more of TEOS compared to the synthesis described in the Experimental Section. Following this line of reasoning, the thickness of the silica shell could also be tuned by using the same amount of TEOS but with varying the amount of QDs. However, with this approach there is still the possibility of forming empty silica nanoparticles if the concentration of QDs in the microemulsion is too low (see the Supporting Information, Figure S3a). In the same way, if the concentration of QDs is too high, it results in the formation of inhomogeneous and sometimes incomplete silica shells (see the Supporting Information, Figure S3b). Thus, for the silica encapsulation of QDs, there is an optimal range of concentrations of these nanocrystals in the microemulsion, which will of course depend on the composition of the microemulsion (i.e., oil:water:surfactant ratios). Once this range of concentrations is found, the thickness of the silica shell is better tuned by adapting the amount of silica precursor.

3.2. Optical Properties. We use in this work "flash" CdSe/CdS QDs with a well-defined and sharp emission peak centered at 630 nm (Figure 2a). The encapsulation of these CdSe/CdS

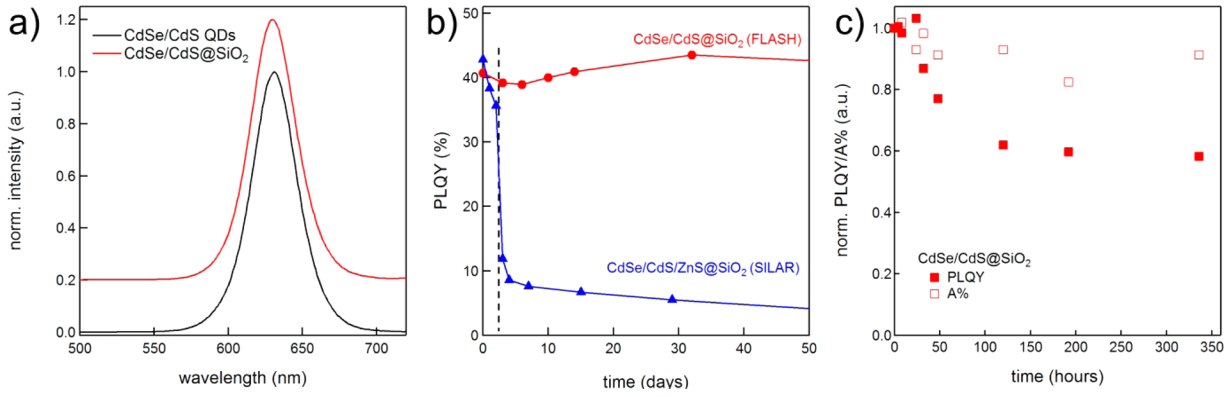

Figure 2. (a) Emission spectra of the CdSe/CdS QDs in toluene and the CdSe/CdS@SiO_2 nanoparticles after 10 months of storage in water (the emission spectra are normalized and slightly offset for clarity). (b) Evolution of the PLQY of the CdSe/CdS@SiO_2 nanoparticles as a function of time and compared to CdSe/CdS/ZnS@SiO_2 nanoparticles where the QDs were prepared by the SILAR method (the dashed line indicates the day the nanoparticles were transferred into water). (c) Evolution of the PLQY (solid symbols) and absorption at 365 nm (A%, open symbols) of a CdSe/CdS@SiO_2 nanoparticles solution in water under continuous UV irradiation (4W UV lamp, λ = 366 nm). In c, the values are normalized to their initial value (t = 0 h).

QDs in silica nanoparticles did not induce any modification in neither the shape nor the position of their emission spectrum, even after more than 10 months of storage in water (Figure 2a). This observation is a first indication of the long-term stability of these nanoparticles in water. Indeed, partial oxidation of the QDs would have resulted in a shift of the emission spectrum toward shorter wavelengths.

3.2.1. Stability of the Photoluminescence Quantum Yield. The absolute PLQY of the CdSe/CdS@SiO_2 nanoparticles was followed carefully in time by using an integrating sphere (see the Supporting Information for a complete description of the method and calculation details) and the values are reported in Figure 2b. As a benchmark, more "conventional" CdSe/CdS/ZnS QDs prepared by the successive ionic layer adsorption and reaction (SILAR) method were also encapsulated in silica through the same microemulsion process (see the Supporting Information, for the synthesis and characterization details). The PLQY of these "SILAR" CdSe/CdS/ZnS@SiO_2 nanoparticles was also followed as a function of time of storage in water and the results are compared with those obtained for "flash" CdSe/CdS@SiO_2 nanoparticles in Figure 2b. The values at days 0 to 2 correspond to measurements of the PLQY during the microemulsion syntheses. On day 3, the nanoparticles were purified by centrifugation and transferred into water. Thus, the values at day 3 are obtained after the nanoparticles have spent no more than a few hours in water. Figure 2b shows that both QDs have an initial PLQY of about 40%. In the case of nanoparticles based on SILAR grown CdSe/CdS/ZnS QDs, Figure 2b shows that their PLQY already decreases significantly during the microemulsion process. Upon transfer into water, the PLQY quickly dropped below 10% and keeps on decreasing with further storage in water. On the other hand, Figure 2b clearly evidence that the nanoparticles based on "flash" CdSe/CdS QDs keep their PLQY unchanged with time. Even after 10 months of storage in water they remained perfectly bright, with a PLQY of about 40%. In addition, the preservation of the PLQY with "flash" QDs appeared to be independent from the silica shell thickness. Indeed, QD@SiO_2 nanoparticles with either very thin or very thick silica shells as those illustrated in Figure 1c, d also retained their PLQY in water. In the case of SILAR-grown QDs, the decrease in PLQY can be explained by the action of the ROS that are present in water. It has been reported that defects in core−shell QDs, such as grain boundaries or incomplete shell layers, act as an inlet for oxygen to reach the core of the QDs.[30] The oxidation of QDs typically results in a deterioration of their optical properties with notably a blue shift of the absorption and emission spectra. In a humid or aqueous environment, this effect is even more critical since the presence of water molecules broadens the lowest unoccupied molecular orbital (LUMO) states of oxygen and therefore facilitate the formation of ROS,[31] which will be even more aggressive toward the QDs and can critically decrease their PLQY. In this regard, "flash" CdSe/CdS QDs, which are synthesized at a relatively high temperature compared to SILAR QDs (330 and about 225 °C, respectively), may have a much better crystallinity and thus a lower defect density resulting in a more efficient protection of the core from ROS. Chen et al. recently reported a method to prepare CdSe/CdS QDs with compact CdS shells through a slow continuous growth, which also retained a high PLQY upon transfer into water.[32] The relatively thick CdS shells might also play an important role in preserving the PLQY of "flash" CdSe/CdS QDs. So-called "giant" CdSe/CdS QDs were already reported to fully retain their PLQY in water,[33] although the present "flash" CdSe/CdS only have about 8 layers of CdS compared to the 15 or more CdS layers in "giant" CdSe/CdS QDs. Thus, both the high crystallinity of the "flash" CdSe/CdS QDs, which are synthesized at high temperature and their relatively thick CdS shells could explain why these QDs are much more resistant than SILAR ones after silica encapsulation and transfer into water.

3.2.2. Silica Passivation of the QDs. When "flash" CdSe/CdS QDs were transferred into water using a S^{2-} ligand exchange procedure, i.e., without any silica encapsulation (see the Supporting Information for details on the procedure), their PLQY immediately dropped to 14%. This critical drop of the PLQY is most likely due to a poor passivation of the surface of the QDs by the sulfur ligands. Thus, the fully preserved PLQY of the QD@SiO_2 nanoparticles indicates that the silica is intimately interacting with the QD surface, resulting in a good passivation and a high PLQY. It is worth noting that the thickness of the silica shell in itself does not play any role in preserving the optical properties. Indeed, CdSe/CdS@SiO_2 nanoparticles with very thin silica shells, such as those illustrated in Figure 1c, also retained a PLQY of about 40% after transfer into water.

3.2.3. Improved Photostability. To further assess the photostability of these "flash" CdSe/CdS@SiO_2 nanoparticles, we continuously irradiated a 3 mL solution of these nanoparticles in water with UV light simply by leaving the solution directly on top of a standard 4W laboratory UV lamp (model Benda NU-4 KL, λ = 366 nm). The solution was prepared so as to have an absorption of ca. 50% at 365 nm across an optical path length of 1 cm. Figure 2c shows the evolution of both the PLQY and the absorption of this solution as a function of the irradiation time. The reported absorption values are those determined directly during the PLQY measurements using an integrating sphere (see the Supporting Information for calculation details). One should note that for every measurement the entire volume of the same solution was systematically analyzed and that its vicinity with the UV lamp typically increased the temperature of the solution to ca. 40 °C. After 1 week of continuous irradiation in these conditions, the PLQY of the QD@SiO_2 nanoparticles solution decreased by about 40% and the absorption by about 15% of their initial values. Longer irradiation periods up to 2 weeks did not result in any further decrease of the PLQY or absorption values. The partial dissolution of the QDs, as indicated by the decrease in the absorption value, induced a shift of the emission spectrum of only 3 nm toward shorter wavelengths (see the Supporting Information, Figure S4). The dissolution of QDs upon UV irradiation is due to their photooxidation, which is a strongly solvent-dependent process.[17] For instance, the same experiment performed on these QDs dispersed in toluene without any silica coating resulted in the dissolution of 80% of the QDs in only a few days, with a concomitantly gradual decrease of their PLQY down to complete extinction (see the Supporting Information, Figure S5), whereas the QDs remained relatively unaffected when they were dispersed in heptane. In this regard, water constitutes a very aggressive solvent as ROS are easily formed due to interactions between water and oxygen molecules. As a matter of fact, when S^{2-}-stabilized "flash" CdSe/CdS QDs were transferred into water using a ligand exchange procedure, they fully dissolved under UV irradiation in a matter of a few tens of minutes (see the Supporting Information, Figure S6). Thus, it appears that the silica

encapsulation does not only provide the QDs with enhanced physicochemical stability, as demonstrated by the fully preserved PLQY after transfer into water, but also with enhanced photostability. Improved photostability was already reported for silica coated CdSe/CdS dot-in rods, which were prepared in a similar way as the "flash" CdSe/CdS dot-in-dots involved in this study.[24] However, even if the silica coating appears to be essential for the photochemical stability of the QD@SiO_2 nanoparticles, it is not a sufficient condition. Indeed, in the case of the CdSe/CdS/ZnS@SiO_2 nanoparticles based on SILAR grown QDs and in spite of the silica shell, the QDs could still dissolve, leaving empty hollow silica nanoparticles behind (see the Supporting Information, Figure S2). Thus, even if the silica shell is of importance, it has to be combined with the good crystallinity of the "flash" CdSe/CdS QDs, which are synthesized at relatively high temperature, to result in CdSe/CdS@SiO_2 nanoparticles with high physicochemical stability and photostability.

3.3. Application to Cell Labeling. As these "flash" CdSe/CdS@SiO_2 nanoparticles constitute promising nanoprobes for bioimaging, several parameters relevant to cell labeling were evaluated in detail, including acute cytotoxicity, qualitative and quantitative uptake of the nanoparticles and their effects on cell morphology. Finally, the functionality of these nanoparticles at nontoxic concentrations for long-term cell visualization by fluorescence microscopy was investigated to have a first, straightforward indication of the suitability of these nanoparticles for cell tracking studies. These results are compared in details with our previous report on the toxicity and cell labeling studies of bare S^{2-}-stabilized "flash" CdSe/CdS QDs.[34]

3.3.1. Toxicity Study. Acute cytotoxic effects of the CdSe/CdS@SiO_2 nanoparticles on HUVEC cells were evaluated and compared to the toxicity of empty SiO_2 nanoparticles of similar size without any inner QD core (see the Supporting Information, Figure S7 for the synthesis and characterization details of these empty SiO_2 nanoparticles). To this end, we used previously optimized methods that assess nanoparticle toxicity under highly reproducible conditions and thus facilitate a comparison of data obtained for other materials (see the Supporting Information for details on the methodology).[26] Figure 3 shows a clear effect of the QD@SiO_2 on the HUVEC viability only at the highest dose of 100 nM, whereas the empty SiO_2 nanoparticles did not elicit any toxic effects over the entire concentration range (2 to 100 nM). Thus, the toxic effect observed in the first case can be solely attributed to the QDs. Previous studies have reported cytotoxic effects of Cd^{2+}-containing core–shell QDs to be noticeable from concentrations of 20 nM on.[20,35] We recently reported that S^{2-}-stabilized "flash" CdSe/CdS QDs were also found to induce cytotoxicity at levels as low as 2 nM.[34] The present results clearly indicate that the silica coating greatly reduces the toxicity of the QDs because the first significant effect appears only at a dose that is 50 times higher than for bare "flash" QDs. This is consistent with other studies where embedding different types of hydrophobic nanomaterials in a silica shell has also been found to enhance their colloidal stability and to reduce their toxicity.[36] Given the rather porous nature of the silica shell, this finding is somewhat surprising, as it would be expected that the bare QDs or silica-coated QDs would be exposed to their final microenvironment to a similar degree and therefore elicit toxicity to a similar extent. This finding is nevertheless in line with the results obtained above, where the CdSe/CdS@SiO_2 nanoparticles in water remained very stable

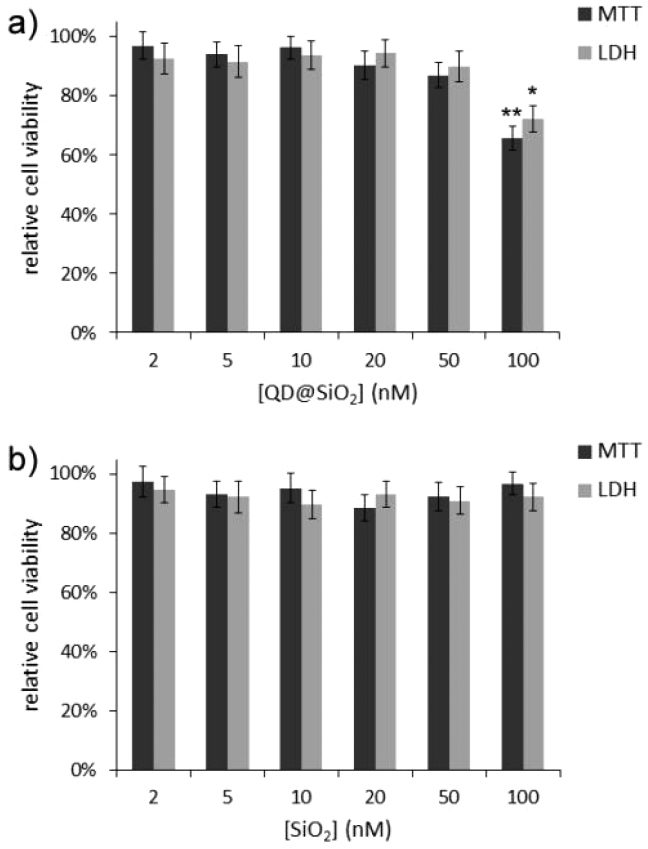

Figure 3. Relative viability of HUVECs cells exposed for 24 h to CdSe/CdS@SiO_2 nanoparticles (a) or SiO_2 nanoparticles (b) at various concentrations and for MTT and LDH assays (*: $p < 0.05$; **: $p < 0.01$).

under continuous UV irradiation, whereas the S^{2-}-stabilized CdSe/CdS dissolved quickly in the same conditions. These preliminary results on the toxicity of "flash" CdSe/CdS@SiO_2 nanoparticles clearly indicate that the CdSe/CdS@SiO_2 nanoparticles could be used for cell labeling at a concentration up to 50 nM.

The stability of the CdSe/CdS@SiO_2 nanoparticles was further demonstrated by performing two complementary control experiments, where the toxicity of free Cd^{2+} ions on C17.2 cells was evaluated (see the Supporting Information, Figure S8). The data reveal clear significant effects on cell viability at levels of 800 nM of free Cd^{2+}. To evaluate whether these levels of Cd^{2+} are representative for the Cd^{2+} levels obtained from the CdSe/CdS@SiO_2 nanoparticles, we also exposed cells to medium that was previously incubated with the nanoparticles for 24 h, after which the nanoparticles were removed by ultracentrifugation. Figure S9 (see the Supporting Information) reveals a clear concentration-dependent effect of Cd^{2+} ions released from the nanoparticles on cell viability, but the extent of the effects compared to the full CdSe/CdS@SiO_2 nanoparticles was much lower. The data reveal that for nanoparticle-derived Cd^{2+} at 50 and 100 nM nanoparticles, similar cell viability levels were obtained as for free Cd^{2+} at 400 and 800 nM, respectively, suggesting low levels of Cd^{2+} release (approximately 8 ions per nanoparticle).

3.3.2. Cellular Uptake. To evaluate the CdSe/CdS@SiO_2 nanoparticles in terms of their potential for cell labeling, we first investigated their cellular uptake. HUVEC cells were incubated with the CdSe/CdS@SiO_2 nanoparticles and 5 μM of 3,3′-

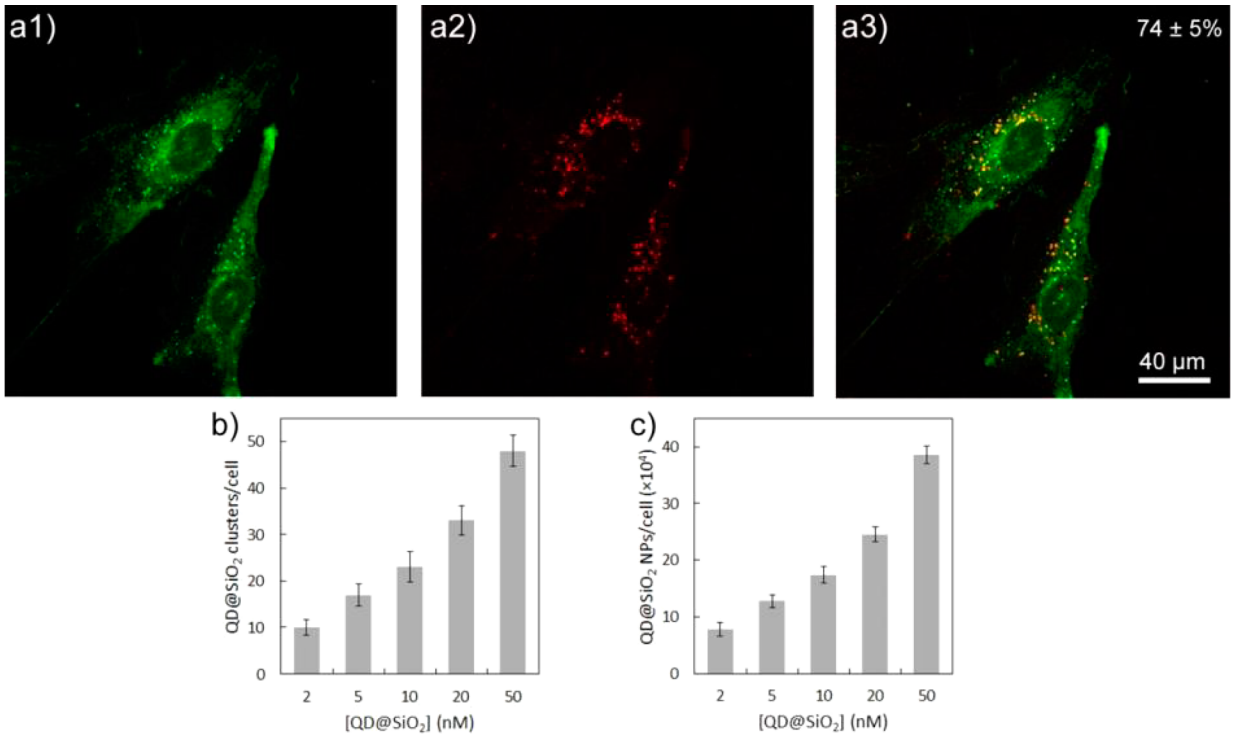

Figure 4. Cellular uptake of the CdSe/CdS@SiO_2 nanoparticles. (a) HUVEC cells were exposed to CdSe/CdS@SiO_2 nanoparticles for 30 min at 50 nM in the presence of the lipophilic dye DiO, which stains the endosomes. The fluorescence images show (a1) the DiO-stained cellular vesicles (green channel), (a2) the emission of the CdSe/CdS@SiO_2 nanoparticles (red channel), and (a3) the merged image. The degree of colocalization is given in the upper hand corner (a3). (b) Number of CdSe/CdS@SiO_2-positive vesicles per HUVEC cell and (c) number of CdSe/CdS@SiO_2 nanoparticles per HUVEC cell upon exposure of HUVECs for 24 h to various nontoxic concentrations of the nanoparticles. Data are expressed as mean ± standard error to the mean (n = 3).

dioctadecyloxacarbocyanine perchlorate (DiO). DiO is a lipophilic dye that can primarily stain endosomal structures when a sufficiently short incubation time is used. Figure 4a reveals a clear colocalization of the green-colored vesicles (endosomes) and red dots (CdSe/CdS@SiO_2 nanoparticles) as assessed by confocal microscopy, indicating that the nanoparticles are internalized by the cell through means of endocytosis and that they reside in endosomal or lysosomal structures, which is common for most types of nanomaterials such as semiconductor QDs,[37] including the bare "flash" CdSe/CdS QDs.[34]

Next, the cellular uptake levels of the CdSe/CdS@SiO_2 nanoparticles were quantified. As a first approximation, the number of nanoparticle-containing clusters (red dots) in an entire cell was counted for a total of 100 cells per condition (Figure 4b). However, when nanoparticles are endocytosed by the cell, they will eventually all localize in a limited number of endosomal structures, which each can contain from a few nanoparticles up to several hundreds or even thousands of them. Therefore, the number of nanoparticle-containing clusters per cell is not very informative from a toxicological point of view as it is impossible to link observed toxicity with actual QD numbers. To determine the actual number of nanoparticles that are internalized per cell, we labeled cells with the CdSe/CdS@SiO_2 nanoparticles, after which 1×10^6 cells were collected and lysed in a low osmotic potassium buffer with alkaline pH (9.8). Upon cell lysis, the nanoparticles are released in the alkaline surroundings and their fluorescence intensity can then be measured spectrofluorometrically to determine their number. Figure 4c shows the average number of CdSe/CdS@SiO_2 nanoparticles taken up by the HUVEC cells, revealing that even at the lowest dose, several tens of thousands of nanoparticles have been internalized. Thus, in addition to low toxicity effects, the CdSe/CdS@SiO_2 also show high cellular uptake levels.

3.3.3. Effect on Cell Morphology. As one of the prime applications of the CdSe/CdS@SiO_2 nanoparticles would be the fluorescent visualization of labeled cells, one aspect that is very important is whether the internalization of the nanoparticles affects cell morphology and whether labeled cells still look identical to unlabeled cells. For this purpose, HUVEC cells were labeled with various concentrations of the CdSe/CdS@SiO_2 nanoparticles after which the cells were stained for α-tubulin and visualized by confocal microscopy. On the basis of these images, the cell spreading (i.e., the surface area covered by a single cell) can be determined as an indication of whether the internalized nanoparticles affect cell morphology. Additionally, cell spreading is an important indication of how "stressed" the cells are. Indeed, it has been shown that cellular geometry is an important indicator and mediator in determining cell life or death.[38] Figure 5 shows well-spread cells in either control conditions (Figure 5a) or when labeled with 10 nM (Figure 5b), 20 nM (Figure 5c), or 50 nM (Figure 5d) of CdSe/CdS@SiO_2 nanoparticles. The internalized nanoparticles show a typical perinuclear localization in the most dense regions of tubulin. On the basis of these images, the nanoparticles do not appear to disturb the tubulin cytoskeleton network. This is in contrast with previous findings on various types of particles, including iron oxide particles, gold particles, and QDs.[35,39,40] High intracellular, but nontoxic, levels of these materials (ranging from 10 nM for QDs to 50 nM for gold particles), all showed to result in cytoskeletal rearrangements. Interestingly,

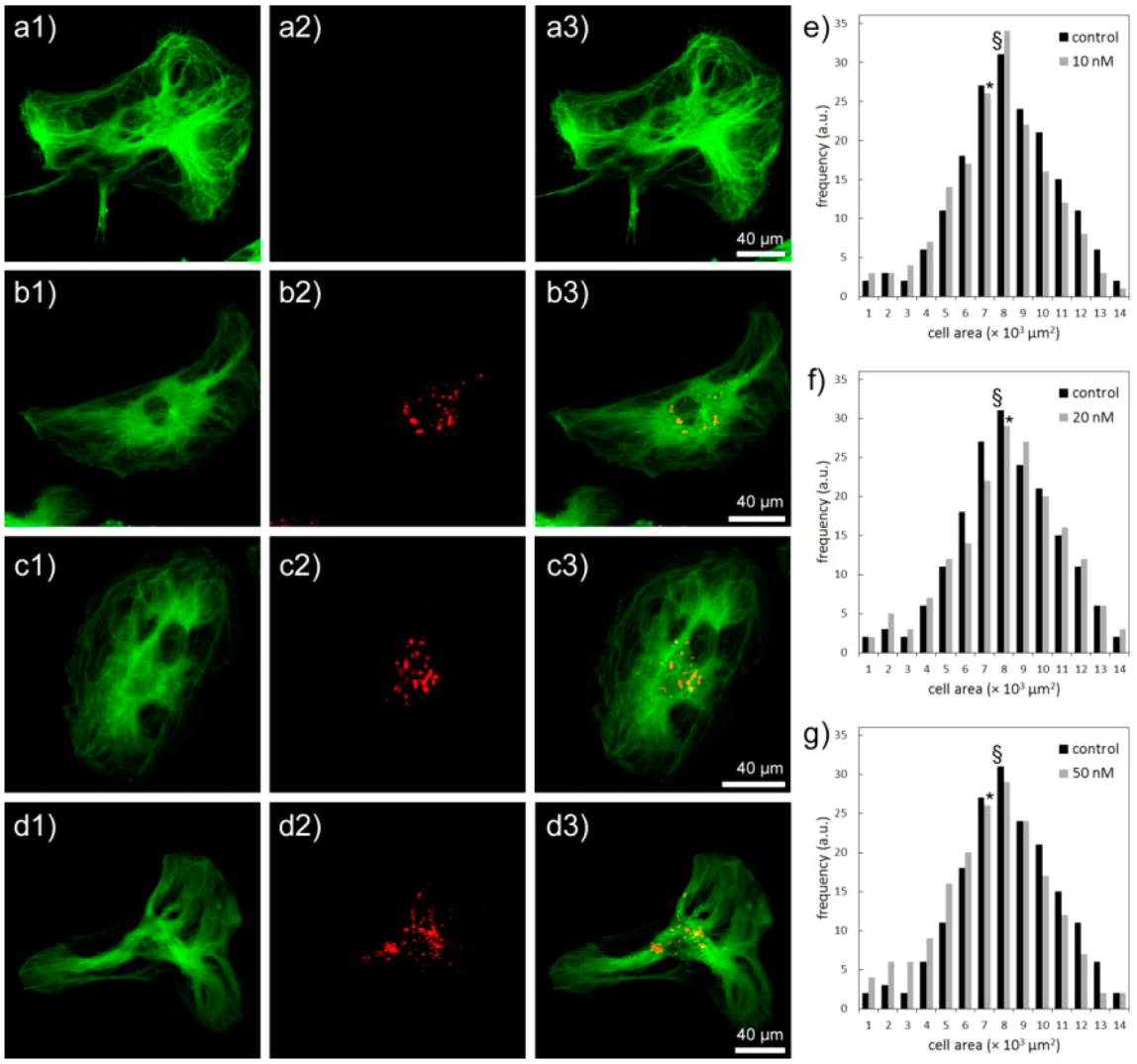

Figure 5. Effect of the CdSe/CdS@SiO_2 nanoparticles on the cell morphology. (a–d) Representative confocal images of HUVEC cells exposed to (a) 0, (b) 10, (c) 20, or (d) 50 nM of CdSe/CdS@SiO_2 nanoparticles for 24 h, where the cells are stained for a-tubulin (left column; green) and show uptake of the CdSe/CdS@SiO_2 nanoparticles (middle column, red). The images in the third column are merged images. (e–g) Histograms showing the cell area of control (dark bars) and CdSe/CdS@SiO_2-treated (light bars) HUVEC cells exposed to the nanoparticles for 24 h at (e) 10, (f) 20, or (g) 50 nM. The average cell area for control cells is indicated by § and for treated cells by *.

in a previous study on dye-doped silica nanoparticles, no cytoskeletal effects were previously observed either,[41] suggesting that the silica coating of the CdSe/CdS@SiO_2 nanoparticles is the dominant factor and overcomes cytotoxic effects that the core QDs would have on the cellular cytoskeleton. The reason behind the protective role of the silica coating is still unclear, and more research is needed to elucidate the precise mechanism at play. When comparing the total cell areas of labeled cells with unlabeled control cells (Figure 5e–g), no distinct difference can be seen between the various conditions, suggesting that at noncytotoxic conditions, the CdSe/CdS@SiO_2 nanoparticles do not affect cell spreading. In comparison, bare "flash" CdSe/CdS QDs were also found not to affect significantly cell spreading but in this case the study was limited to lower concentrations due to their higher toxicity.[34] The results reported here on high concentrations of CdSe/CdS@SiO_2 nanoparticles clearly indicate that they can be efficiently used for fluorescent visualization of live cells.

3.3.4. Long-Term Cell Visualization. One key aspect in evaluating the potential of functional nanoparticles is how long they can be efficiently visualized in live (dividing) cells. To this end, HUVEC cells were labeled with various nontoxic concentrations of the CdSe/CdS@SiO_2 nanoparticles, after which the cells were allowed to grow in culture and divide. At several points, small samples of the cells were taken and visualized by fluorescence microscopy to look for the presence of the nanoparticles (Figure 6a). On the basis of these images, the percentage of cells which contain at least one clearly distinguishable cluster of CdSe/CdS@SiO_2 nanoparticles is then calculated. Figure 6b reveals that even for the lowest concentration of CdSe/CdS@SiO_2 nanoparticles (10 nM), the cells can easily be visualized for up to 5 cell divisions with more than 50% of them being still positive for nanoparticles, before the majority of them loses their fluorescent labels due to dilution effects and possible degradation of the nanoparticles.[42,43] In addition, for the highest tested concentration (50 nM), more than 50% of the cells remain efficiently labeled with nanoparticles after 9 cell divisions, which is a considerably long period of time for QD based nanoprobes.[35] This long duration signifies that (1) the CdSe/CdS@SiO_2 nanoparticles

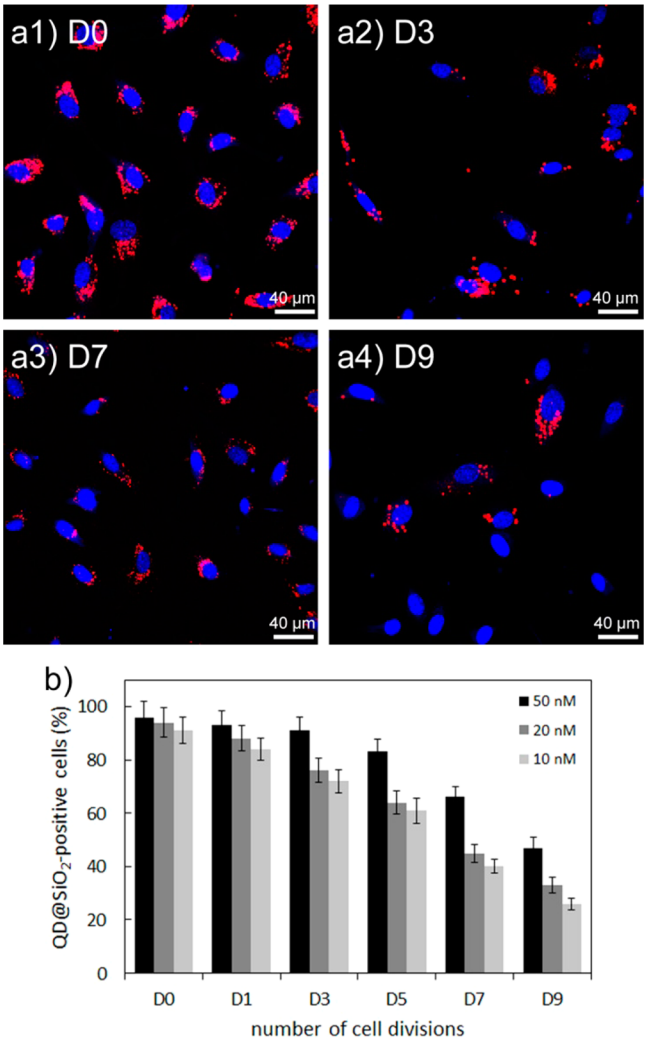

Figure 6. Efficacy of the CdSe/CdS@SiO_2 nanoparticles for long-term cell visualization. (a) Representative fluorescence images of HUVEC cells exposed to CdSe/CdS@SiO_2 nanoparticles for 24 h at 50 nM. Images are taken after cells have undergone (a1) 0, (a2) 3, (a3) 7, or (a4) 9 cell divisions. The CdSe/CdSe@SiO_2 nanoparticles appear as red and the cell nuclei are counterstained in blue by DAPI. (b) Percentage of HUVEC cells containing CdSe/CdS@SiO_2 nanoparticles relative to the entire population of HUVEC cells. Cells were labeled for 24 h with CdSe/CdS@SiO_2 nanoparticles at 10 nM (light gray), 20 nM (medium gray), or 50 nM (dark gray) after which they were kept in culture and representative samples were collected after cells had undergone 0, 1, 3, 5, 7, or 9 cell divisions. Data are expressed as mean ± SEM (n = 3).

themselves are not very toxic as high initial levels can be tolerated without any cytotoxic effects, (2) the emission properties of the nanoparticles appear to be relatively unaffected by the endosomal environment to which they are exposed. This is in clear contrast with bare "flash" CdSe/CdS QDs, which were found to quickly release Cd^{2+} ions in the cells and could not be visualized for more than 2 cell divisions.[34]

4. CONCLUSION

In conclusion, we demonstrate that "flash" CdSe/CdS QDs as synthesized using a seeded growth method at high temperature are very efficient light emitters for biolabeling applications. They can be encapsulated in silica nanoparticles through a water-in-oil microemulsion process, with a high control on the morphology of the nanoparticles and the thickness of the silica shell. This silica coating provides the nanocrystals with enhanced colloidal stability in polar solvents, while fully preserving their optical properties. Indeed, the PLQY of the nanoparticles remains high and unchanged even after several months of storage in water. They also showed greatly improved photostability in water under continuous UV irradiation compared to bare QDs. This enhanced stability of the optical properties, which were thoroughly investigated using an integrating sphere, is a key parameter in the development of QDs based luminescent nanoprobes as it determines their potential for bioimaging applications. In addition, the silica shell successfully reduced the cytotoxicity of the QDs, with first significant effects on HUVEC cell viability appearing only at concentrations 50 times higher than for bare QDs. The potential of these CdSe/CdS@SiO_2 nanoparticles for cell labeling was evidenced by fluorescence confocal microscopy showing their rapid and high endosomal uptake by HUVEC cells. Furthermore, thanks to their reduced toxicity and to the high stability of their optical properties, these CdSe/CdS@SiO_2 nanoparticles appeared to be particularly useful for long-term cell visualization, with nanoparticles identifiable by confocal microscopy for up to 9 cell divisions. Taken together these data clearly demonstrate the extensive potential of these nanoparticles for biomedical applications. Possibly thanks to their high crystallinity, alloyed interfaces and relatively thick CdS shells, "flash" QDs have a higher physicochemical stability and photostability than other QDs synthesized using more common strategies such as the SILAR method. Additionally, the presence of the silica shell provides an important level of protection against environmentally induced degradation of the QDs, making these "flash" CdSe/CdS@SiO_2 nanoparticles highly efficient luminescent markers with powerful optical properties combined with low toxicity levels. Their further development into even more complex architectures will lead to highly functional tools for advanced applications such as intracellular imaging and theranostics.

■ ASSOCIATED CONTENT

Ⓢ Supporting Information

Details on measurement and calculation of the PLQY, synthesis and characterization of the CdSe/CdS/ZnS@SiO_2 nanoparticles based on SILAR grown QDs, additional characterizations on "flash" CdSe/CdS QDs and CdSe/CdS@SiO_2 nanoparticles, synthesis and characterization of the empty SiO_2 nanoparticles, methodology for toxicity and cell labeling studies, data of free Cd^{2+} and nanoparticle-devoid media on cell viability. This material is available free of charge via the Internet at http://pubs.acs.org.

■ AUTHOR INFORMATION

Corresponding Authors

*E-mail: tangi.aubert@ugent.be.
*E-mail: zeger.hens@ugent.be.

Present Address

⊥S.J.S. is currently at Department of Medicine, Biomedical NMR Unit, KU Leuven, Herestraat 49, 3000 Leuven, Belgium.

Notes

The authors declare no competing financial interest.

■ ACKNOWLEDGMENTS

The authors acknowledge BelSPo (IAP 7.35, photonics@be), FWO-Vlaanderen (Project G.0760.12; KaN 1509012N), Ghent University (BOF12/GOA/015) and Hercules Foundation (project AUGE/09/024 "Advanced Luminescence Setup") for financial support.

■ REFERENCES

(1) Pelaz, B.; Jaber, S.; de Aberasturi, D. J.; Wulf, V.; Aida, T.; de la Fuente, J. M.; Feldmann, J.; Gaub, H. E.; Josephson, L.; Kagan, C. R.; Kotov, N. A.; Liz-Marzán, L. M.; Mattoussi, H.; Mulvaney, P.; Murray, C. B.; Rogach, A. L.; Weiss, P. S.; Willner, I.; Parak, W. J. The State of Nanoparticle-Based Nanoscience and Biotechnology: Progress, Promises, and Challenges. *ACS Nano* **2012**, *6*, 8468−8483.

(2) Niemeyer, C. M. Nanoparticles, Proteins, and Nucleic Acids: Biotechnology Meets Materials Science. *Angew. Chem., Int. Ed.* **2001**, *40*, 4128−4158.

(3) Zhang, L.; Gu, F. X.; Chan, J. M.; Wang, A. Z.; Langer, R. S.; Farokhzad, O. C. Nanoparticles in Medicine: Therapeutic Applications and Developments. *Clin. Pharmacol. Ther.* **2008**, *83*, 761−769.

(4) Michalet, X.; Pinaud, F. F.; Bentolila, L. A.; Tsay, J. M.; Doose, S.; Li, J. J.; Sundaresan, G.; Wu, A. M.; Gambhir, S. S.; Weiss, S. Quantum Dots for Live Cells, in Vivo Imaging, and Diagnostics. *Science* **2005**, *307*, 538−544.

(5) Medintz, I. L.; Uyeda, H. T.; Goldman, E. R.; Mattoussi, H. Quantum Dot Bioconjugates for Imaging, Labelling and Sensing. *Nat. Mater.* **2005**, *4*, 435−446.

(6) Xing, Y.; Xia, Z.; Rao, J. Semiconductor Quantum Dots for Biosensing and In Vivo Imaging. *IEEE Trans. Nanobiosci.* **2009**, *8*, 4−12.

(7) Chan, W. C. W.; Maxwell, D. J.; Gao, X.; Bailey, R. E.; Han, M.; Nie, S. Luminescent Quantum Dots for Multiplexed Biological Detection and Imaging. *Curr. Opin. Biotechnol.* **2002**, *13*, 40−46.

(8) Mulvaney, P.; Liz-Marzan, L. M.; Giersig, M.; Ung, T. Silica Encapsulation of Quantum Dots and Metal Clusters. *J. Mater. Chem.* **2000**, *10*, 1259−1270.

(9) Gerion, D.; Pinaud, F.; Williams, S. C.; Parak, W. J.; Zanchet, D.; Weiss, S.; Alivisatos, A. P. Synthesis and Properties of Biocompatible Water-Soluble Silica-Coated CdSe/ZnS Semiconductor Quantum Dots. *J. Phys. Chem. B* **2001**, *105*, 8861−8871.

(10) Darbandi, M.; Thomann, R.; Nann, T. Single Quantum Dots in Silica Spheres by Microemulsion Synthesis. *Chem. Mater.* **2005**, *17*, 5720−5725.

(11) Koole, R.; van Schooneveld, M. M.; Hilhorst, J.; de Mello Donegá, C.; Hart, D. C.; van Blaaderen, A.; Vanmaekelbergh, D.; Meijerink, A. On the Incorporation Mechanism of Hydrophobic Quantum Dots in Silica Spheres by a Reverse Microemulsion Method. *Chem. Mater.* **2008**, *20*, 2503−2512.

(12) Selvan, S. T.; Tan, T. T.; Ying, J. Y. Robust, Non-Cytotoxic, Silica-Coated CdSe Quantum Dots with Efficient Photoluminescence. *Adv. Mater.* **2005**, *17*, 1620−1625.

(13) Guerrero-Martínez, A.; Pérez-Juste, J.; Liz-Marzán, L. M. Recent Progress on Silica Coating of Nanoparticles and Related Nanomaterials. *Adv. Mater.* **2010**, *22*, 1182−1195.

(14) Yan, J.; Estévez, M. C.; Smith, J. E.; Wang, K.; He, X.; Wang, L.; Tan, W. Dye-Doped Nanoparticles for Bioanalysis. *Nano Today* **2007**, *2*, 44−50.

(15) Knopp, D.; Tang, D.; Niessner, R. Review: Bioanalytical Applications of Biomolecule-Functionalized Nanometer-Sized Doped Silica Particles. *Anal. Chim. Acta* **2009**, *647*, 14−30.

(16) Zhang, Y.; He, J.; Wang, P.-N.; Chen, J.-Y.; Lu, Z.-J.; Lu, D.-R.; Guo, J.; Wang, C.-C.; Yang, W.-L. Time-Dependent Photoluminescence Blue Shift of the Quantum Dots in Living Cells: Effect of Oxidation by Singlet Oxygen. *J. Am. Chem. Soc.* **2006**, *128*, 13396−13401.

(17) Manner, V. W.; Koposov, A. Y.; Szymanski, P.; Klimov, V. I.; Sykora, M. Role of Solvent−Oxygen Ion Pairs in Photooxidation of CdSe Nanocrystal Quantum Dots. *ACS Nano* **2012**, *6*, 2371−2377.

(18) Wang, Y.; Tang, Z.; Correa-Duarte, M. A.; Pastoriza-Santos, I.; Giersig, M.; Kotov, N. A.; Liz-Marzán, L. M. Mechanism of Strong Luminescence Photoactivation of Citrate-Stabilized Water-Soluble Nanoparticles with CdSe Cores. *J. Phys. Chem. B* **2004**, *108*, 15461−15469.

(19) Chen, N.; He, Y.; Su, Y.; Li, X.; Huang, Q.; Wang, H.; Zhang, X.; Tai, R.; Fan, C. The Cytotoxicity of Cadmium-Based Quantum Dots. *Biomaterials* **2012**, *33*, 1238−1244.

(20) Kirchner, C.; Liedl, T.; Kudera, S.; Pellegrino, T.; Muñoz Javier, A.; Gaub, H. E.; Stölzle, S.; Fertig, N.; Parak, W. J. Cytotoxicity of Colloidal CdSe and CdSe/ZnS Nanoparticles. *Nano Lett.* **2004**, *5*, 331−338.

(21) Hardman, R. A Toxicologic Review of Quantum Dots: Toxicity Depends on Physicochemical and Environmental Factors. *Environ. Health Perspect.* **2006**, *114*, 165−172.

(22) Cirillo, M.; Aubert, T.; Gomes, R.; Van Deun, R.; Emplit, P.; Biermann, A.; Lange, H.; Thomsen, C.; Brainis, E.; Hens, Z. Flash Synthesis of CdSe/CdS Core−Shell Quantum Dots. *Chem. Mater.* **2014**, *26*, 1154−1160.

(23) Aubert, T.; Grasset, F.; Mornet, S.; Duguet, E.; Cador, O.; Cordier, S.; Molard, Y.; Demange, V.; Mortier, M.; Haneda, H. Functional Silica Nanoparticles Synthesized by Water-in-Oil Microemulsion Processes. *J. Colloid Interface Sci.* **2010**, *341*, 201−208.

(24) Pietra, F.; van Dijk-Moes, R. J. A.; Ke, X.; Bals, S.; Van Tendeloo, G.; de Mello Donega, C.; Vanmaekelbergh, D. Synthesis of Highly Luminescent Silica-Coated CdSe/CdS Nanorods. *Chem. Mater.* **2013**, *25*, 3427−3434.

(25) Li, J. J.; Wang, Y. A.; Guo, W.; Keay, J. C.; Mishima, T. D.; Johnson, M. B.; Peng, X. Large-Scale Synthesis of Nearly Monodisperse CdSe/CdS Core/Shell Nanocrystals Using Air-Stable Reagents via Successive Ion Layer Adsorption and Reaction. *J. Am. Chem. Soc.* **2003**, *125*, 12567−12575.

(26) Soenen, S. J.; Rivera-Gil, P.; Montenegro, J.-M.; Parak, W. J.; De Smedt, S. C.; Braeckmans, K. Cellular Toxicity of Inorganic Nanoparticles: Common Aspects and Guidelines for Improved Nanotoxicity Evaluation. *Nano Today* **2011**, *6*, 446−465.

(27) Carbone, L.; Nobile, C.; De Giorgi, M.; Sala, F. D.; Morello, G.; Pompa, P.; Hytch, M.; Snoeck, E.; Fiore, A.; Franchini, I. R.; Nadasan, M.; Silvestre, A. F.; Chiodo, L.; Kudera, S.; Cingolani, R.; Krahne, R.; Manna, L. Synthesis and Micrometer-Scale Assembly of Colloidal CdSe/CdS Nanorods Prepared by a Seeded Growth Approach. *Nano Lett.* **2007**, *7*, 2942−2950.

(28) de Mello, J. C.; Wittmann, H. F.; Friend, R. H. An Improved Experimental Determination of External Photoluminescence Quantum Efficiency. *Adv. Mater.* **1997**, *9*, 230−232.

(29) Blechinger, J.; Bauer, A. T.; Torrano, A. A.; Gorzelanny, C.; Bräuchle, C.; Schneider, S. W. Uptake Kinetics and Nanotoxicity of Silica Nanoparticles Are Cell Type Dependent. *Small* **2013**, *9*, 3970−3980.

(30) van Sark, W. G. J. H. M.; Frederix, P. L. T. M.; Bol, A. A.; Gerritsen, H. C.; Meijerink, A. Blueing, Bleaching, and Blinking of Single CdSe/ZnS Quantum Dots. *ChemPhysChem* **2002**, *3*, 871−879.

(31) Pechstedt, K.; Whittle, T.; Baumberg, J.; Melvin, T. Photoluminescence of Colloidal CdSe/ZnS Quantum Dots: The Critical Effect of Water Molecules. *J. Phys. Chem. C* **2010**, *114*, 12069−12077.

(32) Chen, O.; Zhao, J.; Chauhan, V. P.; Cui, J.; Wong, C.; Harris, D. K.; Wei, H.; Han, H.-S.; Fukumura, D.; Jain, R. K.; Bawendi, M. G. Compact High-Quality CdSe−CdS Core−Shell Nanocrystals with Narrow Emission Linewidths and Suppressed Blinking. *Nat. Mater.* **2013**, *12*, 445−451.

(33) Chen, Y.; Vela, J.; Htoon, H.; Casson, J. L.; Werder, D. J.; Bussian, D. A.; Klimov, V. I.; Hollingsworth, J. A. Giant" Multishell CdSe Nanocrystal Quantum Dots with Suppressed Blinking. *J. Am. Chem. Soc.* **2008**, *130*, 5026−5027.

(34) Soenen, S. J.; Abe, S.; Manshian, B. B.; Aubert, T.; Hens, Z.; De Smedt, S. C.; Braeckmans, K. The Effect of Intracellular Degradation on Cytotoxicity and Cell Labeling Efficacy of Inorganic Ligand-Stabilized Colloidal CdSe/CdS Quantum Dots. *J. Biomed. Nanotechnol.* **2014**, in press.

(35) Soenen, S. J.; Demeester, J.; De Smedt, S. C.; Braeckmans, K. The Cytotoxic Effects of Polymer-Coated Quantum Dots and Restrictions for Live Cell Applications. *Biomaterials* **2012**, *33*, 4882−4888.
(36) Zhang, T.; Stilwell, J. L.; Gerion, D.; Ding, L.; Elboudwarej, O.; Cooke, P. A.; Gray, J. W.; Alivisatos, A. P.; Chen, F. F. Cellular Effect of High Doses of Silica-Coated Quantum Dot Profiled with High Throughput Gene Expression Analysis and High Content Cellomics Measurements. *Nano Lett.* **2006**, *6*, 800−808.
(37) Cho, S. J.; Maysinger, D.; Jain, M.; Röder, B.; Hackbarth, S.; Winnik, F. M. Long-Term Exposure to CdTe Quantum Dots Causes Functional Impairments in Live Cells. *Langmuir* **2007**, *23*, 1974−1980.
(38) Chen, C. S.; Mrksich, M.; Huang, S.; Whitesides, G. M.; Ingber, D. E. Geometric Control of Cell Life and Death. *Science* **1997**, *276*, 1425−1428.
(39) Soenen, S. J. H.; Himmelreich, U.; Nuytten, N.; De Cuyper, M. Cytotoxic Effects of Iron Oxide Nanoparticles and Implications for Safety in Cell Labelling. *Biomaterials* **2011**, *32*, 195−205.
(40) Soenen, S. J.; Manshian, B.; Montenegro, J. M.; Amin, F.; Meermann, B.; Thiron, T.; Cornelissen, M.; Vanhaecke, F.; Doak, S.; Parak, W. J.; De Smedt, S.; Braeckmans, K. Cytotoxic Effects of Gold Nanoparticles: A Multiparametric Study. *ACS Nano* **2012**, *6*, 5767−5783.
(41) Soenen, S. J.; Manshian, B.; Doak, S. H.; De Smedt, S. C.; Braeckmans, K. Fluorescent Non-Porous Silica Nanoparticles for Long-Term Cell Monitoring: Cytotoxicity and Particle Functionality. *Acta Biomater.* **2013**, *9*, 9183−9193.
(42) Zhu, Z.-J.; Yeh, Y.-C.; Tang, R.; Yan, B.; Tamayo, J.; Vachet, R. W.; Rotello, V. M. Stability of Quantum Dots in Live Cells. *Nat. Chem.* **2011**, *3*, 963−968.
(43) Summers, H. D.; Rees, P.; Holton, M. D.; Rowan Brown, M.; Chappell, S. C.; Smith, P. J.; Errington, R. J. Statistical Analysis of Nanoparticle Dosing in a Dynamic Cellular System. *Nat. Nanotechnol.* **2011**, *6*, 170−174.